



LEHIGH
University

Characterization of Cyclic Inelastic Strain Behavior On Properties of A572 Gr. 50 and A913 Gr. 50 Rolled Sections

**E.J. Kaufmann
B. Metrovich
A.W. Pense**

**Final Report
to
American Institute of Steel Construction**

ATLSS Report No. 01-13

December 2001

**ATLSS is a National Center for Engineering Research
on Advanced Technology for Large Structural Systems**

117 ATLSS Drive
Bethlehem, PA 18015-4729

Phone: (610)758-3525
Fax: (610)758-5902

www.atlss.lehigh.edu
Email: inatl@lehigh.edu

TABLE OF CONTENTS

TABLE OF CONTENTS	i
LIST OF FIGURES	ii
LIST OF TABLES	iv
ACKNOWLEDGEMENT	v
I. INTRODUCTION	1
I.1 Research Objective and Approach	1
I.2 Background	1
II. EXPERIMENTAL PROGRAM	2
II.1 Properties of As-Rolled Sections	2
II.2 Effect of Inelastic Straining on Tensile Properties	3
II.2.1 Test Procedure	3
II.2.2 Test Results	3
II.2.3 Strain Aging Effects	3
II.3 Effect of Inelastic Straining on CVN Properties	4
II.3.1 Test Procedure	4
II.3.2 Test Results	4
II.3.3 Strain Aging Effects	4
II.4 Cyclic Strain Behavior	4
II.4.1 Test Procedure	4
II.4.2 Test Results	5
II.4.3 Low Cycle Fatigue Tests	5
III. SUMMARY AND CONCLUSIONS	6
IV. REFERENCES	7

LIST OF FIGURES

Figure 1 - Effect of Straining and Aging on Tensile Properties of Steel.	15
Figure 2 – Prestrain Coupon and Test Specimen Layout.	16
Figure 3A – Stress-Strain Curves for Steel A for Various Pre-Strain Conditions	17
Figure 3B – Stress-Strain Curves for Steel B for Various Pre-Strain Conditions	17
Figure 3C – Stress-Strain Curves for Steel C for Various Pre-Strain Conditions	18
Figure 3D– Stress-Strain Curves for Steel D for Various Pre-Strain Conditions	18
Figure 4 – Summary of Yield and Tensile Strength vs. Strain Condition	19
Figure 5 – Summary of Tensile Ductility vs. Strain Condition	19
Figure 6A – CVN Transition Curves (TL) for Steel A for Various Pre-Strain Conditions	20
Figure 6B - CVN Transition Curves (LT) for Steel A for Various Pre-Strain Conditions	20
Figure 6C - CVN Transition Curves (TL) for Steel B for Various Pre-Strain Conditions	21
Figure 6D - CVN Transition Curves (LT) for Steel B for Various Pre-Strain Conditions	21
Figure 6E - CVN Transition Curves (TL) for Steel C for Various Pre-Strain Conditions	22
Figure 6F - CVN Transition Curves (LT) for Steel C for Various Pre-Strain Conditions	22
Figure 6G - CVN Transition Curves (TL) for Steel D for Various Pre-Strain Conditions	23
Figure 6H - CVN Transition Curves (LT) for Steel D for Various Pre-Strain Conditions	23
Figure 7 – $\Delta T_{\text{transition}}$ at 15 ft-lbs From As-rolled Condition for Various Pre-strain Conditions	24
Figure 8 – Cyclic Strain Test Specimen (ASTM E606)	24
Figure 9 – Cyclic Strain Test Set-up	25
Figure 10 – Typical Strain-Time Plot for a Single Cyclic Strain Test	25
Figure 11A – Cyclic Strain Behavior of Steel A (10 cycles at 2%, 4%, 6% and 8% Strain Range)	26
Figure 11B – Cyclic Strain Behavior of Steel B (10 cycles at 2%, 4%, 6% and 8% Strain Range)	26

Figure 11C – Cyclic Strain Behavior of Steel C (10 cycles at 2%, 4%,6% and 8% Strain Range)	27
Figure 11D – Cyclic Strain Behavior of Steel D (10 cycles at 2%, 4%,6% and 8% Strain Range)	27
Figure 12 – Comparison of Monotonic and Stabilized Cyclic Stress-Strain Behavior for the Four Steels	28
Figure 13 – Strain-Life Plot for Steel C (A572 Gr. 50) Extrapolated to Low Fatigue Life	29

LIST OF TABLES

TABLE 1 – Tensile Properties of Test Materials	8
TABLE 2 – Chemical Compositions	9
TABLE 3A – CVN Test Results (Steel A)	10
TABLE 3B – CVN Test Results (Steel B)	12
TABLE 3C – CVN Test Results (Steel C)	13
TABLE 3D – CVN Test Results (Steel D)	14

ACKNOWLEDGEMENT

The authors wish to acknowledge the support of the American Institute of Steel Construction and the Pennsylvania Infrastructure Technology Alliance (PITA) in performing this project. Also acknowledged are Nucor-Yamato Steel Co., Trade Arbed Inc., and British Steel for providing material for the study through SAC Joint Venture.

I. INTRODUCTION

In a series of cracking incidents that have occurred during fabrication with rolled column shapes [1] it was found that the cracking originated in the k-area of the column. It was also found that the mechanical properties in this area were substantially changed as a result of the rotary straightening process now widely used in manufacturing rolled shapes. The cold deformation introduced in the web near the web-flange intersection (k-area) during rotary straightening of the section was found to have markedly elevated the yield and tensile strength with concomitant decreases in ductility and fracture toughness [2]. The local elevation in strength and reduction in ductility and toughness in the k-area was believed to have been a key factor in the cause for the cracking. Beyond the fabrication precautions that have now been implemented to mitigate future cracking in this region [3] the subsequent service performance of rolled sections containing these low ductility and toughness regions, particularly under severe service conditions as occurs in earthquakes, also needs to be examined. The study reported herein is one of four studies initiated by the American Institute of Steel Construction to address these needs.

I.1 RESEARCH OBJECTIVE AND APPROACH

The objective of the current study was to examine the basic mechanical properties of inelastically strained A572 Gr. 50, A913 Gr. 50 and A36 steel sections to provide test data that could be used to assess the effects of manufacturing straightening procedures on the notch toughness and ductility of the k-region of rolled shapes. An A36 section was included in the study to compare the inelastic strain behavior of a section produced earlier by integrated mills to sections produced by current manufacturing practices. The studies included tensile and Charpy-V-notch properties (ASTM E8 and E23) of the as-rolled sections and at three levels of monotonic pre-strain (2%, 8%, 12%). Limited studies of the effects of strain aging were also conducted.

Although the strain conditions introduced in the k-area during rotary straightening are predominantly shear with small tensile and compressive components, quantitative simulation of these complex conditions in the laboratory is not readily achievable. Consequently, monotonic tensile straining was chosen to approximate these conditions and to compare the steels and observe trends at different strain levels. Considering the relatively large magnitudes of inelastic strains proposed the difference in loading on the net effect on properties may be small.

The cyclic inelastic strain behavior of the materials under tension-compression loading was also studied using standard strain controlled fatigue test methodologies (ASTM E606). The contemporary Gr.50 sections were W14 X 176 sections produced by three different mills. Two sections were A572 Gr. 50 and the third was A913 Gr. 50. The A36 steel was a W36 X 260 section manufactured prior to 1984 and was believed to be produced by an integrated mill.

I.2 BACKGROUND

The strain hardening of structural steel has been shown to produce changes in the hardness, strength, ductility, and toughness of the steel. The phenomena of strain aging can produce additional changes in these properties. The effect of these processes on the mechanical properties of steel is

illustrated in Figure 1. If, after initial inelastic deformation to Point A on the stress-strain curve of a steel specimen the load is removed a certain amount of permanent deformation remains as a pre-strain. If reloaded immediately the specimen loads elastically to Point A again and continues to extend as if it had not been unloaded. If the specimen is unloaded and aged at room temperature or at moderately elevated temperatures the lower yield point and lower yield extension returns again but at an elevated stress than occurred upon immediate reloading (Point A). Subsequent extension to failure will often be accompanied by a slight increase in tensile strength and reduction in total elongation of the specimen. Straining followed by subsequent aging not only results in increased yield point and reduction in tensile ductility in some steels but also affects the notch toughness of the steel. Reductions in absorbed energy and upward shifts in transition temperature occur in steels as a result of straining often with further changes following aging.

The potential for increases in yield and tensile strength along with decreases in ductility and toughness after monotonic straining have been demonstrated in A572, A588A, A588B, A737B and A737C plates [4]. In this study cold strain at the level of 5 to 10% increased yield strengths of the steels by over 200% and subsequent aging at 370 C raised them another 25%. Cold strain increased the 34 J Charpy V-notch transition temperature by 25-50 F with aging increasing the transition temperature modestly above the as-strained level.

More recently, limited studies of rotary straightened structural members has demonstrated that the k-area of some wide flange shapes have substantially increased hardness, yield and tensile strengths with accompanied decreases in tensile ductility and notch toughness. Hardness as high as RB 97 and notch toughness as low as 4J (3 ft-lbs) at room temperature have been reported in this region [1,2].

II. EXPERIMENTAL PROGRAM

II.1 PROPERTIES OF AS-ROLLED SECTIONS

The as-rolled properties of the A572 Gr. 50, A913 Gr.50 and A36 rolled sections as well as the mill report test results are summarized in Table 1. Standard 0.505 in. round specimens located at the web mid-thickness and centerline of the section were prepared for each section. In general, the tensile properties of the A572 Gr. 50 steel (Steels A and C) were consistent with the mill certificates, however, the A913 Gr. 50 steel (Steel B) provided somewhat lower strengths which can be attributed to the mid-thickness positioning of the 0.505 in. test specimen compared to the full thickness coupon tested by the mill.

Chemical composition of the steels including residual elements are given in Table 2. The analyses show that the steels satisfy their respective specification requirements within product analysis tolerances. Residual element levels in Steels A, B, and C are at typical levels found in modern day structural steel sections. The very low residual element levels measured in the A36 section (Steel D) provided additional evidence of its integrated mill origin.

II.2 EFFECT OF INELASTIC PRE-STRAINING ON TENSILE PROPERTIES

II.2.1 Test Procedure

To study the effects of inelastic strain on the mechanical properties of the various steels large (35" x 4") full web thickness tensile coupons were prepared located near the web centerline of the sections (see Figure 2). Material in this region was sufficiently removed from the k-area so as to be least affected by rotary straightening of the section and thus represented as close to the as-rolled condition as possible. For each of the four rolled sections coupons were monotonically pre-strained in tension to three different levels of strain (2%, 8%, and 12%) from which longitudinal 0.505 in. tensile specimens and L-T (Longitudinal-Transverse) and T-L (Transverse-Longitudinal) oriented Charpy V-notch specimens were then fabricated as also shown in Figure 2. Additional coupons were prepared from Steel A and pre-strained to an intermediate strain (8%) for subsequent aging (10 hours) at 200 F and 400 F. Punch marks were placed at regular intervals within the reduced section and measured after pre-straining to verify that the pre-strain was distributed uniformly within this region.

II.2.2 Test Results

Figures 3A through 3D show the stress-strain behavior obtained for the four steels (A, B, C, and D) initially (as-rolled) and at the various pre-strains. The results, summarized in Figure 4 and 5, shows that all of the contemporary steels followed the same general trend. With increasing pre-strain the yield point increased by 20-40% approaching the tensile strength of the steel while tensile elongation decreased by about the same magnitude. The effect of pre-strain on tensile strength was less (10-20% increase). In contrast, the yield point of the A36 steel (Steel D) increased by over 100% at the highest pre-strain with tensile strength approaching the Gr. 50 steels under similar pre-strains.

At 12 % pre-strain, close to strain at ultimate tensile strength in the as-rolled condition, yield points and tensile strengths of all four steels were nearly identical as the strain hardening capacity of the steel was fully exhausted by the pre-strain. It is interesting that the near absence of further strain hardening after a 12% pre-strain closely resembles the stress-strain behavior of tensile specimens removed from the k-area of rotary straightened sections [2]. This suggests that the k-areas of rotary straightened sections undergo a magnitude of deformation comparable to at least a 12% monotonic tensile pre-strain.

II.2.3 Strain Aging Effects

Aging of Steel A pre-strained to 8% strain resulted in only a small additional increase in strength (-2%). Considering the low carbon (0.067%) and nitrogen (0.0032%) levels measured in this steel it is not surprising that its strain aging response was small. It is interesting that low nitrogen levels were found in all of the steels (see Table 2) and well below the A992 manufacturer's limit of 0.012%. A588 plate steels with higher nitrogen levels (0.011-0.012) studied by Herman et al [4] showed greater effect of strain aging particularly on CVN properties.

II.3 EFFECT OF INELASTIC PRE-STRAINING ON CVN PROPERTIES

II.3.1 Test Procedure

Standard Charpy V-notch specimens were fabricated from the same large pre-strained coupons as the tensile specimens. Eighteen L-T and T-L oriented test specimens (see Figure 2) were each fabricated for the three pre-strain levels and in the as-rolled condition. The specimens were tested in triplicate over a range of temperatures within the transition temperature range for the material.

II.3.2 Test Results

Results of Charpy V-notch (CVN) tests over the transition temperature range are shown for the as-rolled and pre-strained sections in Figures 6A through 6H and tabulated in Tables 3A through 3D. All three contemporary sections (Steels A, B, and C) exhibited upper shelf behavior at room temperature in the as-rolled condition whereas the earlier produced A36 (Steel D) exhibited room temperature toughness in the transition temperature range. Pre-straining resulted in progressive reductions in absorbed energy and an upward shift in transition temperature. A summary of the shift in the 15 ft-lb transition temperature relative to the as-rolled condition ($\Delta T_{\text{transition}}$) is provided in Figure 7. For the three contemporary steel sections a pre-strain of 2% was found to shift the 15 ft-lb transition temperature 10-25 F. At 12% pre-strain the shift ranged from 40-100 F. Transverse oriented specimens consistently experienced a larger shift in transition temperature at all pre-strain levels. This is also consistent with the orientation of cracks which have developed in the k-area.

At the largest pre-strain of 12% the CVN absorbed energy at 70 F for the three contemporary steels was about 20 ft-lbs which is greater than CVN energies that have been measured in the k-area of rotary straightened sections (ie. about 5 ft-lbs) [1,2] and suggests that k-area deformations are greater than is introduced by a monotonic tensile strain of 12%.

II.3.3 Strain Aging Effects

As with tensile properties the effect of an elevated temperature aging treatment on notch toughness was also small. An increase in transition temperature of about 15 F was observed for Steel A at the higher aging temperature of 400 F compared to 68 F increase observed by Herman et al [4].

II.4 CYCLIC STRAIN BEHAVIOR

II.4.1 Test Procedure

Cyclic strain tests following ASTM E606 [5] methodology were carried out on all four materials. The 0.375 in. dia. round test specimen design utilized is shown in Figure 7. The surface finish of the reduced section of the test specimens was a 16 μm finish. Figure 8 shows a test specimen installed in the 55 kip servohydraulic load frame used with a 1 in. gage length extensometer attached to the reduced section of the test specimen. Tests were conducted at four strain range levels

of 2%, 4%, 6% and 8%. Each test consisted of 10 tension-compression cycles at a single strain range. The specimens were loaded at a constant displacement rate of 0.005 in./min. to the specified strain range. A typical strain-time plot for a single test is shown in Figure 9.

II.4.2 Test Results

Figures 10A through 10D show a composite plot of the four individual tests performed at each strain range for the four steels. The plots show that all four materials cyclically strain hardened in a similar manner. At the lowest strain range of 2% cyclic stabilization occurred within 4-5 cycles. At the higher strain ranges all four steels cyclically stabilized within 2-3 cycles.

The similarity in the cyclic strain hardening characteristics of the steels is further demonstrated in Figure 11. The stabilized cyclic stress-strain test data for each strain range is plotted along with the corresponding monotonic stress-strain curves for comparison. The stabilized cyclic stress-strain data was fitted to an equation of the form $\sigma = K \epsilon^n$ where n is the cyclic strain hardening exponent. This material property is typically in the range of 0.1-0.2 for steels. In general, materials with higher cyclic strain hardening exponents tend to exhibit greater low cycle fatigue resistance. Steels A, B, and C yielded nearly the same strain hardening exponent ranging from 0.096-0.111. Steel D exhibited a higher value for n of 0.150. This is consistent with the lower strength and higher ductility of A36 steel compared to the other steels.

It is noteworthy that for the large inelastic strain cycles studied the majority of the strain hardening in all four steels occurred during the first strain cycle. This suggests that the majority of the strain damage is introduced during this initial cycle and that the monotonic pre-strains used to measure effects on properties likely represents the bulk of the strain damage.

II.4.3 Low Cycle Fatigue Tests

No visual indications of cracking was observed in any of the materials within the ten applied cycles. To obtain information on crack initiation behavior a limited number of additional tests were performed where cycling was continued until initiation of fatigue cracking. Three tests were conducted at a strain range of 2%, 6% and 8% using Steel C. Cracking developed at 370 cycles at the lowest applied strain range and within 25 cycles at 8% strain range. A strain-life plot of the results is shown in Figure 12. Although a limited number of tests were performed the results can be used to estimate the strain range required to initiate cracking for the number of cycles typically applied during rotary straightening of rolled sections. As discussed earlier the tension-compression strain cycles used to simulate the deformation cycles introduced during rotary straightening provide only estimates of the magnitude of strain range required to develop cracking. Rotary straightening normally applies five to ten cycles to the k-areas of a rolled section. Extrapolating the curve in Figure 12 to shorter fatigue life suggests that cracking in the k-area could be expected at strain ranges of 13-18% for the number of strain cycles applied in rotary straightening.

III.SUMMARY AND CONCLUSIONS

1. The behavior of contemporary A 572 Gr. 50 and A913 Gr.50 rolled sections under monotonic inelastic tensile straining was found to be similar. Inelastic tensile strains ranging from 2-12% resulted in similar changes in tensile and notch toughness properties in all three contemporary steels studied. Yield and tensile strengths increased by 20-40% and 10-20%, respectively, with concomitant reductions in tensile elongations of 15-50%. Elevation of CVN transition temperature ranged from 20-70 F over the range of strains studied. Larger shifts in transition temperature were observed transverse to the strain (and rolling) direction ranging from 15-100 F.
2. The effect of inelastic tensile strain on the mechanical properties of an A36 rolled section produced prior to 1984 was largely similar to contemporary Gr. 50 rolled sections with the exception that larger relative changes in yield strength and tensile ductility were measured compared to contemporary Gr. 50 steel. For an equivalent level of tensile pre-strain, however, the yield and tensile strength remained below that of Gr. 50 steels with higher tensile ductility.
3. Strain aging effects were found to be small in A572 Gr. 50 rolled sections. For 8% tensile prestrain a 2% increase in strength and 15 F increase in transition temperature was observed. Carbon and nitrogen levels were low in all four steels studied which may account for the small strain aging response.
4. The cyclic inelastic strain behavior of all three contemporary Gr. 50 steels was also similar. Cyclic stabilization was achieved after 2-3 applied strain cycles for strain ranges above 2%. The cyclic inelastic strain behavior of A36 steel produced prior to 1984 indicated a higher low cycle fatigue resistance consistent with its lower strength and higher ductility.
5. Low cycle fatigue cracking was not observed in any of the steels examined at strain ranges as high as 8 % in 10 applied tension-compression strain cycles. Limited tests using A572 Gr. 50 suggested that tension-compression strain ranges of at least 13-18% are necessary for crack initiation to occur in 5-10 cycles normally applied in rotary straightening.
6. Comparison of the tensile and CVN properties of pre-strained A572 Gr. 50 and A913 Gr. 50 sections and properties of the k-area of similar rotary straightened sections suggests that the k-region properties of rotary straightened sections possess properties comparable to monotonic tensile pre-strains of at least 12%.

IV. REFERENCES

1. Tide, R.H.R., "Evaluation of Steel Properties and Cracking in "k"-area of W Shapes", Engineering Structures, Vol. 22, 2000, pp. 128-134.
2. "AISC Materials and Design Workshop, January 8, 1997, Chicago, IL", AISC, 1997.
3. "AISC Advisory Statement on Mechanical Properties Near the Fillet of Wide Flange Shapes and Interim Recommendations, January 10, 1997, Modern Steel Construction, AISC, February 1997.
4. Herman, W.A. ,Erazo, M.A., DePatto, L.R., Sekizawa, M., and Pense, A.W., "Strain Aging Behavior of Microalloyed Steels", WRC Bulletin 322, Welding Research Council, April 1987.
5. ASTM E606-92 "Standard Practice for Strain-Controlled Fatigue Testing", Vol. 03.01, ASTM, 2000.

TABLE 1
 PROPERTIES OF TEST MATERIALS

Steel Code	Member Size	Grade	Y.S. (ksi)	T.S. (ksi)	Y/T	Elong.(2") (%)	Red. Area (%)
A	W14 X 176	A572 Gr. 50	58.03 [60.37]*	76.17 [78.66]	0.76	34.5 [27]	76.9
B	W14 X 176	A913 Gr. 50	51.08 [64.82]	70.25 [79.75]	0.73	37.8 [24]	73.0
C	W14 X 176	A572 Gr. 50	54.25 [55.00]	72.28 [75.00]	0.75	35.5 [23]	72.7
D	W36 X 260	A36	36.13	62.62	0.58	44.6	59.5

Notes: Standard 0.505" round specimens
 Web centerline location
 * Mill Test Report

TABLE 2 CHEMICAL COMPOSITIONS

Element	Composition, wt%			
	Steel A	Steel B	Steel C	Steel D
C	0.067	0.085	0.072	0.17
Mn	1.51	1.20	1.48	0.75
P	0.022	0.023	0.014	0.020
S	0.005	0.020	0.016	0.024
Si	0.28	0.18	0.21	0.05
Cr	0.028	0.11	0.061	0.044
Ni	0.23	0.11	0.13	0.031
Mo	0.065	0.072	0.086	0.038
Al	0.032	0.002	0.002	0.002
Cu	0.31	0.22	0.29	0.021
Co	<0.001	0.010	0.008	0.004
Nb	0.003	0.008	0.003	0.002
Ti	0.002	0.001	0.001	<0.001
V	0.15	0.005	0.057	0.004
W	<0.001	<0.001	<0.001	<0.001
Pb	0.006	0.003	0.011	0.003
Sn	0.004	0.013	0.013	0.002
As	0.003	0.011	0.007	0.005
Zr	0.001	0.001	0.001	<0.001
Ca	<0.001	<0.001	<0.001	<0.001
Sb	0.0034	0.0044	0.0047	<0.0001
B	<0.0001	0.0002	<0.0001	<0.0001
N	0.0032	0.0033	0.0040	<0.0005
Fe	97.3	97.9	97.5	98.8

TABLE 3A CVN TEST RESULTS (STEEL A)

STEEL A

T-L ORIENTATION

Initial Properties		2% pre-strain		8% pre-strain		8% pre-strain 200°F		8% pre-strain 400°F		12% pre-strain	
Temp (F)	CVN (ft-lbs)	Temp (F)	CVN (ft-lbs)	Temp (F)	CVN (ft-lbs)	Temp (F)	CVN (ft-lbs)	Temp (F)	CVN (ft-lbs)	Temp (F)	CVN (ft-lbs)
72	237.5	32	199.5	72	93	72	141	72	107	72	26
72	138	32	116.5	72	111	72	109	72	87	72	110
72	237.5	32	99.5	72	35	72	101	72	63	72	74
32	87	0	36	32	61.5	120	70	120	82	120	101
32	54	0	57	32	39	120	123	120	106	120	89
32	141	0	10	32	20	120	166	120	108	120	107
0	98.5	72	148.5	0	5	32	74	32	41	32	21
0	118.5	72	153.5	0	6.5	32	90.5	32	30	32	8
0	91.5	72	70.5	0	29.5	32	11	32	38	32	46
-40	12	-40	61	-40	18.5	0	26	0	33	0	6
-40	50.5	-40	44.5	-40	5.5	0	28	0	26	0	8.5
-40	17	-40	34	-40	4	0	35	0	35	0	11
-60	11.5	120	136.5	120	112	180	146	180	133.5	180	155
-60	6	120	208	120	117	180	155	180	144	180	150.5
-60	8.5	120	151.5	120	52.5	180	143	180	154	180	132
-80	7	-60	21	180	143.5	-40	7	-40	4		
-80	26	-60	14	180	143.5	-40	5	-40	6		
-80	15	-60	5.5	180	135	-40	20	-40	4.5		

TABLE 3A CVN TEST RESULTS (STEEL A)

STEEL A

L-T ORIENTATION

Initial Properties		2% pre-strain		8% pre-strain		8% pre-strain 200°F		8% pre-strain 400°F		12% pre-strain	
Temp (F)	CVN (ft-lbs)	Temp (F)	CVN (ft-lbs)	Temp (F)	CVN (ft-lbs)	Temp (F)	CVN (ft-lbs)	Temp (F)	CVN (ft-lbs)	Temp (F)	CVN (ft-lbs)
-20	82	32	28	72	237.5	72	231	72	150	72	221
-20	34	32	237	72	237.5	72	215	72	35	72	203
-20	200.5	32	20	72	237.5	72	231	72	17	72	237
32	236.5	0	15	32	212	32	95	120	233	32	109
32	236	0	237	32	21	32	23.5	120	167.5	32	86
32	236.5	0	149.5	32	16	32	99	120	161	32	166
0	236.5	72	237	0	20.5	0	6.5	32	28	0	32.5
0	236.5	72	237	0	124	0	10	32	31.5	0	19
0	54	72	237	0	20	0	65	32	92	0	72
-40	19.5	-40	4.5	-40	10.5	52	194	0	5	-40	6
-40	22	-40	15	-40	19	52	148.5	0	7	-40	7
-40	14	-40	7.5	-40	16	52	13	0	11.5	-40	6
-60	13	-60	7.5	-60	4	-40	8	180	237		
-60	5.5	-60	104	-60	8	-40	6	180	235		
-60	11.5	-60	8.5	-60	3	-40	14	180	234		
-80	32	52	239	52	226			52	126.5		
-80	24	52	235	52	239			52	141		
-80	10	52	239	52	33			52	41		

TABLE 3B CVN TEST RESULTS (STEEL B)

STEEL B

T-L ORIENTATION

Initial Properties		2% pre-strain		8% pre-strain		12% pre-strain	
Temp (F)	CVN (ft-lbs)	Temp (F)	CVN (ft-lbs)	Temp (F)	CVN (ft-lbs)	Temp (F)	CVN (ft-lbs)
72	49.5	32	48.5	72	37.5	72	21
72	51	32	43.5	72	33.5	72	20
72	50	32	37.5	72	32.5	72	22.5
32	43.5	0	25.5	32	13	120	28
32	46	0	25	32	20.5	120	29
32	46.5	0	23	32	16.5	120	29
0	41	72	53	0	16	32	11.5
0	29	72	49.5	0	6	32	9
0	34	72	53.5	0	6	32	13
-40	18.5	-40	14	-40	7	0	5
-40	16	-40	14	-40	5.5	0	7
-40	16.5	-40	17	-40	4.5	0	7
-60	12.5	-60	8	120	37	180	34
-60	13	-60	6.5	120	37.5	180	35
-60	7.5	-60	8.5	120	41.5	180	33.5
-100	3.5					-40	4
-100	2					-40	4
-100	2					-40	4

STEEL B

L-T ORIENTATION

Initial Properties		2% pre-strain		8% pre-strain		12% pre-strain	
Temp (F)	CVN (ft-lbs)	Temp (F)	CVN (ft-lbs)	Temp (F)	CVN (ft-lbs)	Temp (F)	CVN (ft-lbs)
72	110	32	127	72	112	72	110
72	114.5	32	108.5	72	115	72	86
72	118.5	32	125	72	114	72	98.5
32	115.5	0	119.5	32	80.5	32	75.5
32	107	0	92	32	92.5	32	80
32	106	0	83.5	32	91.5	32	88
0	82	72	121.5	0	18	0	15
0	97	72	132	0	19	0	15
0	96	72	119	0	81	0	30
-40	69	-40	29	-40	5	-40	8
-40	35	-40	74	-40	7.5	-40	8
-40	75.5	-40	24.5	-40	8.5	-40	19
-60	50.5	-60	8.5	-60	4.5		
-60	33	-60	33	-60	3.5		
-60	29	-60	9.5	-60	7.5		
-100	7						
-100	4.5						
-100	2.5						

TABLE 3C CVN TEST RESULTS (STEEL C)

STEEL C

T-L ORIENTATION

Initial Properties		2% pre-strain		8% pre-strain		12% pre-strain	
Temp (F)	CVN (ft-lbs)	Temp (F)	CVN (ft-lbs)	Temp (F)	CVN (ft-lbs)	Temp (F)	CVN (ft-lbs)
72	63.5	32	19	72	26.5	72	21
72	54	32	24	72	26	72	21
72	54	32	24.5	72	28	72	18.5
32	36	0	21.5	32	21	120	27
32	36	0	15.5	32	18.5	120	29
32	32	0	21	32	18	120	31
0	26.5	72	45	0	6	32	14
0	22	72	41.5	0	15.5	32	14.5
0	27	72	46.5	0	6	32	5
-40	18	-40	6	-40	3	0	5
-40	14.5	-40	9	-40	4	0	6.5
-40	12.5	-40	9.5	-40	4	0	5
-60	9.5	120	65	120	37.5	180	48
-60	8.5	120	63.5	120	37.5	180	45
-60	6	120	64.5	120	41	180	46
120	66			180	56		
120	66			180	58		
120	64.5			180	58		

STEEL C

L-T ORIENTATION

Initial Properties		2% pre-strain		8% pre-strain		12% pre-strain	
Temp (F)	CVN (ft-lbs)	Temp (F)	CVN (ft-lbs)	Temp (F)	CVN (ft-lbs)	Temp (F)	CVN (ft-lbs)
72	116	32	87.5	72	90.5	72	93.5
72	110.5	32	57.5	72	102.5	72	73.5
72	110	32	87	72	89.5	72	90
32	77	0	34.5	32	82	120	96
32	95.5	0	45.5	32	54	120	98.5
32	66	0	38.5	32	32	120	99
0	40.5	72	116.5	0	34.5	32	36.5
0	36	72	115	0	33	32	15.5
0	68	72	97.5	0	6.5	32	34
-40	24.5	-40	4	-40	3.5	0	6
-40	8	-40	5	-40	4	0	10
-40	35	-40	4.5	-40	5	0	6
-60	4.5	120	123.5	120	103	-40	4
-60	20	120	118	120	106	-40	4
-60	4	120	117	120	102	-40	4
120	121.5			180	102		
120	125			180	101		
120	115			180	110		

TABLE 3D CVN TEST RESULTS (STEEL D)

STEEL D

T-L ORIENTATION

Initial Properties		2% pre-strain		8% pre-strain		12% pre-strain	
Temp (F)	CVN (ft-lbs)	Temp (F)	CVN (ft-lbs)	Temp (F)	CVN (ft-lbs)	Temp (F)	CVN (ft-lbs)
68	29	74	21	74	13.5	74	12.5
68	31	74	20	74	13	74	14.5
68	30	74	21	74	13	74	10
32	17	32	10.5	32	7	32	6
32	20	32	8	32	8.5	32	5
32	19	32	10.5	32	7.5	32	7
0	11	0	7.5	0	6	0	5
0	11	0	5	0	4.5	0	6
0	7	0	6.5	0	6.5	0	3.5
120	34	120	31	120	23	120	15.5
120	36	120	33	120	23	120	16
120	35	120	45	120	25	120	18
160	37	160	34.5	160	29.5	160	23
160	37	160	33	160	27	160	22
160	36	160	35	160	27.5	160	23

STEEL D

L-T ORIENTATION

Initial Properties		2% pre-strain		8% pre-strain		12% pre-strain	
Temp (F)	CVN (ft-lbs)	Temp (F)	CVN (ft-lbs)	Temp (F)	CVN (ft-lbs)	Temp (F)	CVN (ft-lb)
68	41.5	73	40	73	33	73	45
68	52	73	35	73	30.5	73	28
68	45	73	45	73	19	73	36
32	32	32	12	32	5.5	32	6.5
32	25	32	10	32	6.5	32	5.5
32	30	32	10.5	32	6	32	6.5
0	7	0	5.5	0	3.5	0	4
0	8	0	5	0	4	0	4.5
0	11	0	5	0	3	0	4
120	74	120	64	120	45.5	120	50
120	75	120	59	120	40	120	48.5
120	76	120	63	120	47	120	48.5
160	78	160	67	160	60	160	51
160	78	160	69.5	160	57.5	160	49
160	78	160	67	160	60	160	50.5

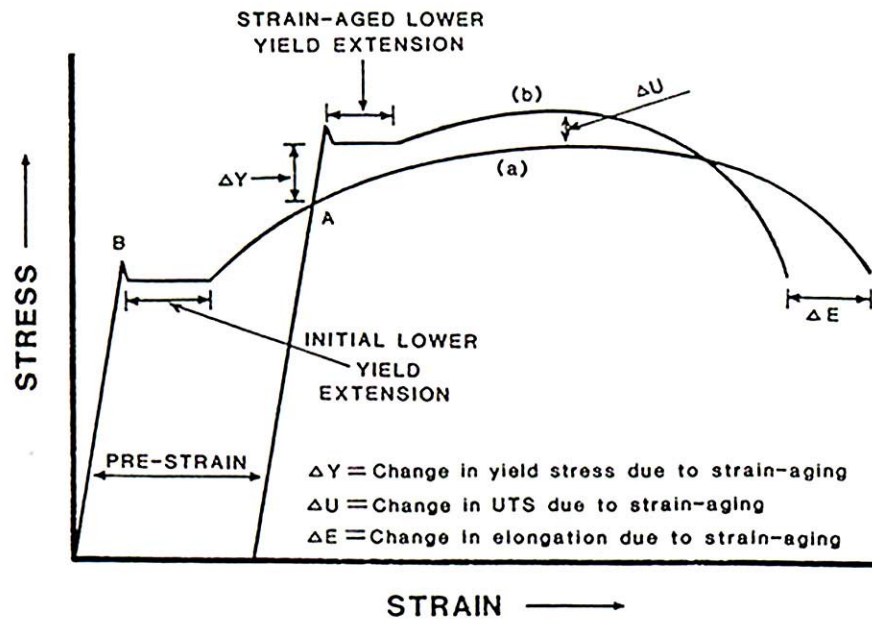


Figure 1 Effect of Straining and Aging on Tensile Properties of Steel.[4]

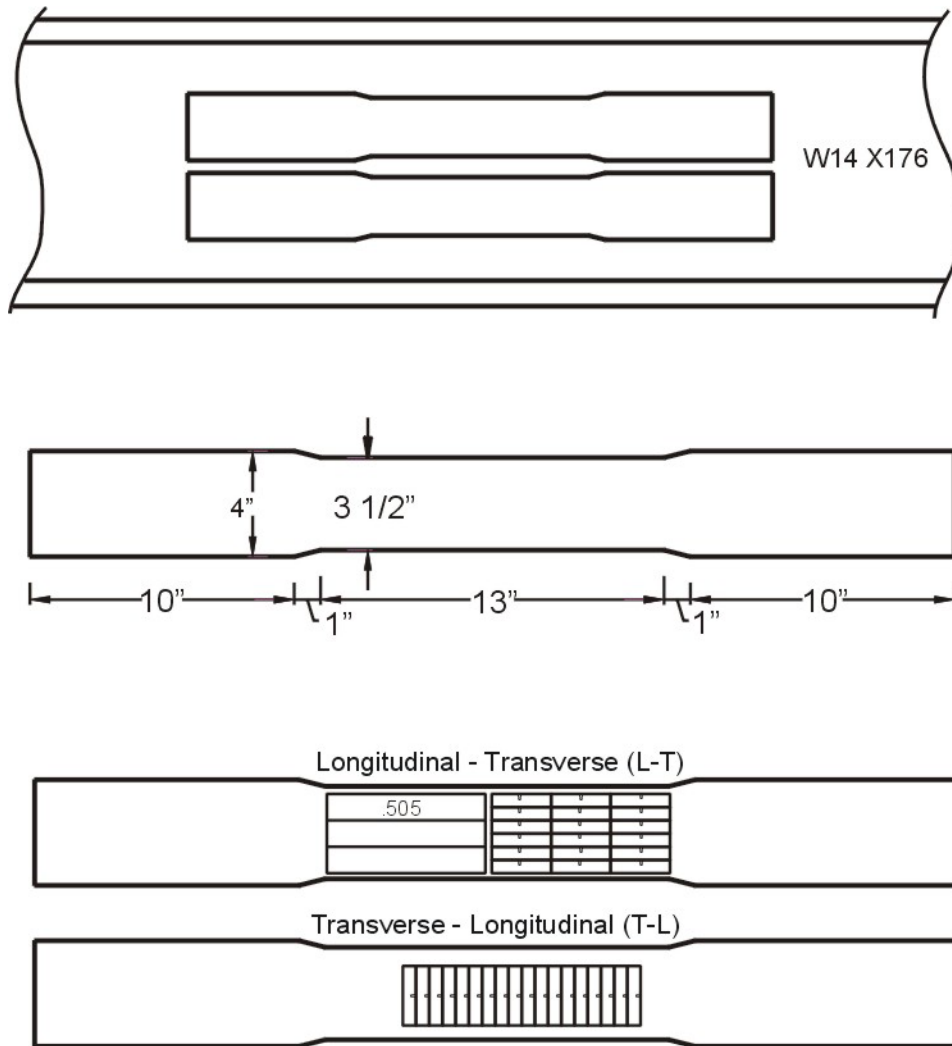


Figure 2 Prestrain Coupon and Test Specimen Layout.

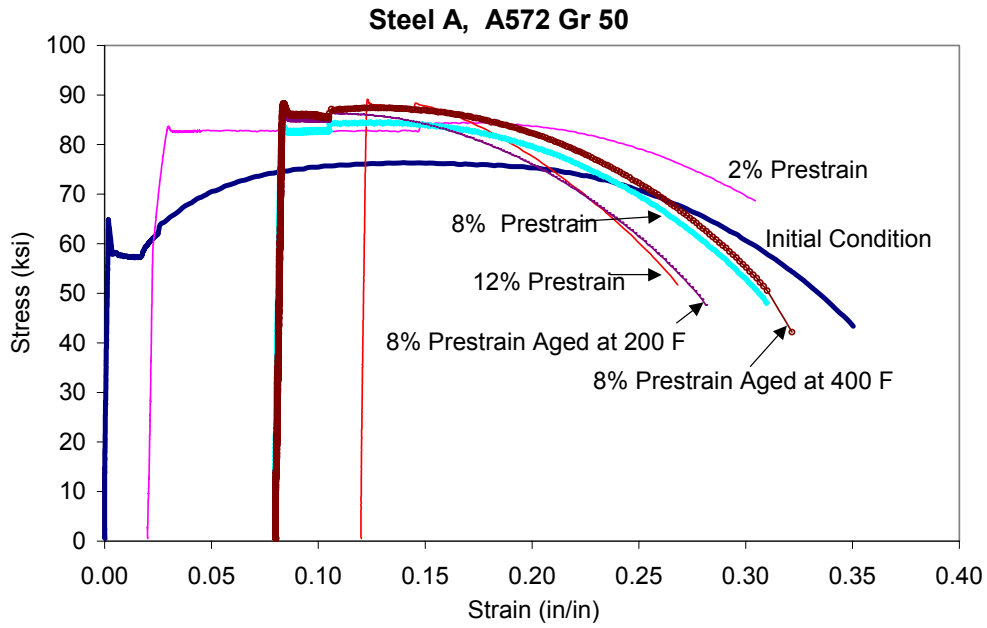


Figure 3A Stress-Strain Curves for Steel A For Various Pre-strain Conditions.

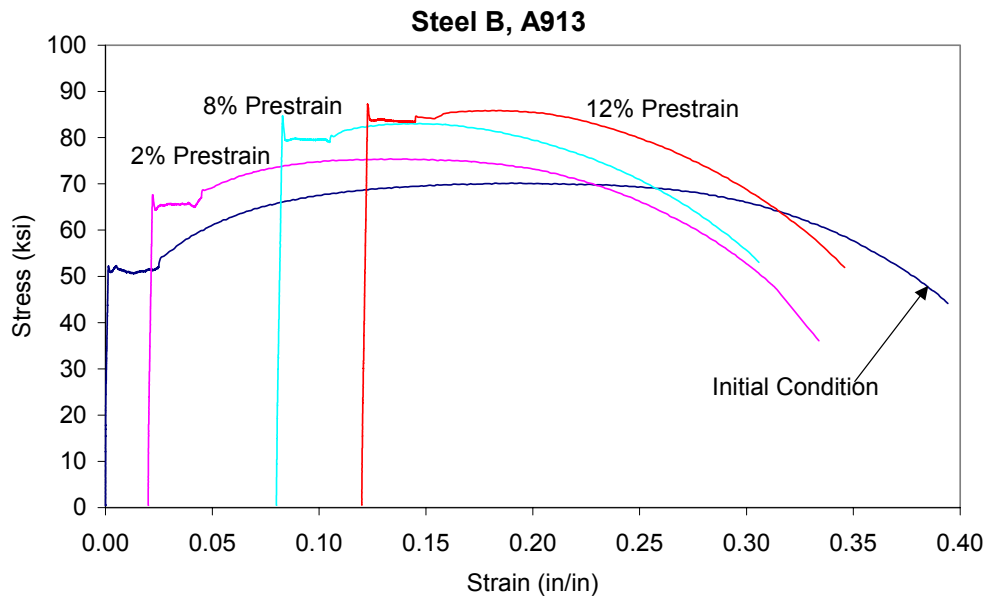


Figure 3B Stress-Strain Curves for Steel B For Various Pre-strain Conditions.

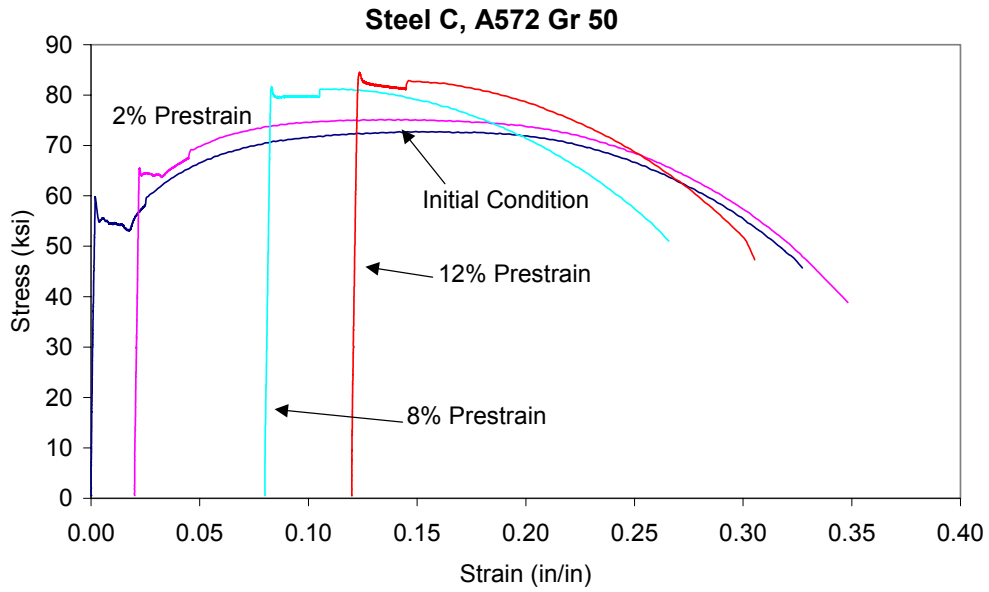


Figure 3C Stress-Strain Curves for Steel C For Various Pre-strain Conditions.

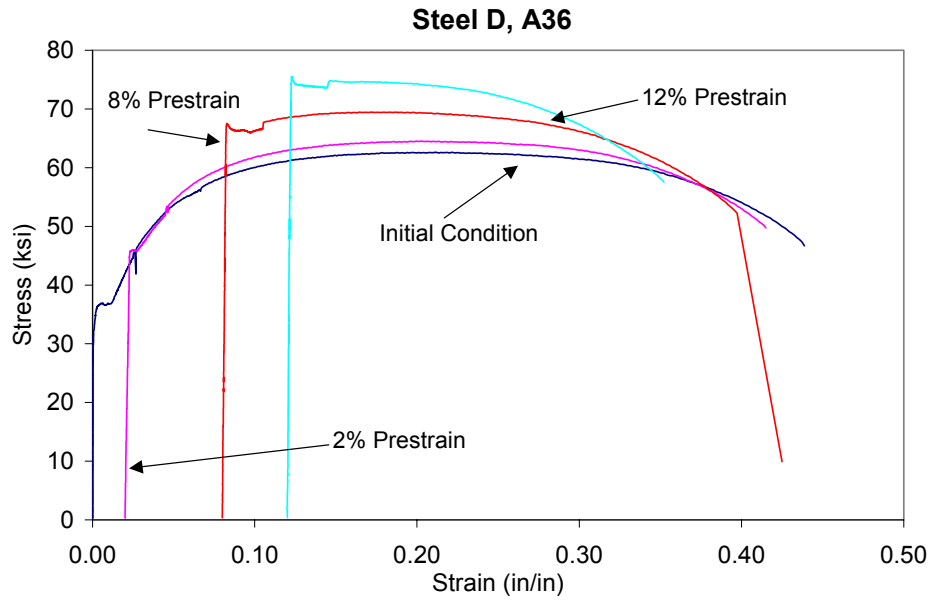


Figure 3D Stress-Strain Curves for Steel D For Various Pre-strain Conditions.

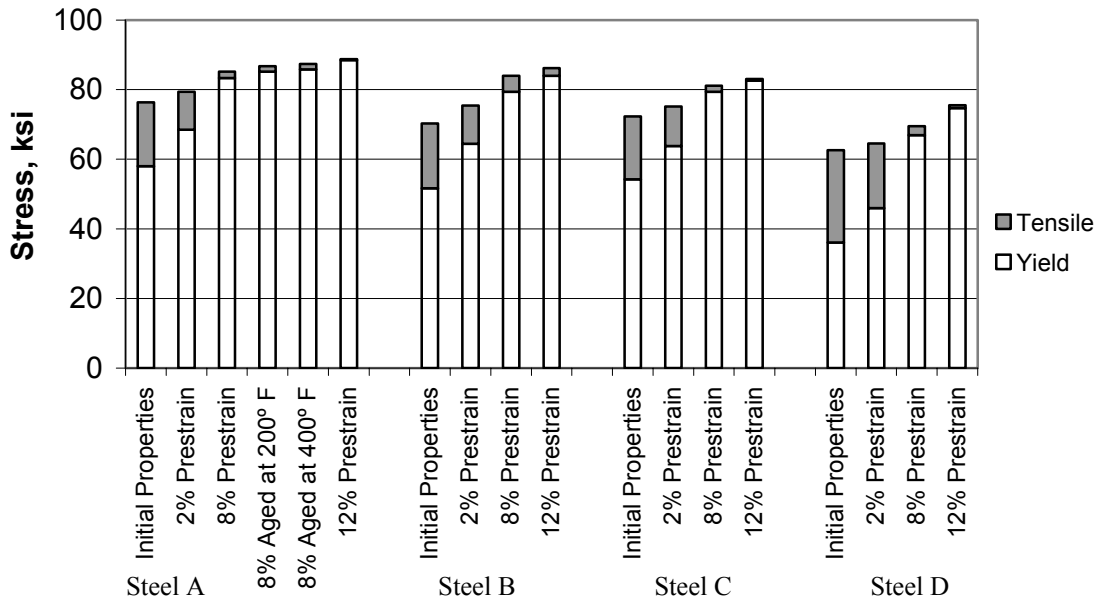


Figure 4 Summary of Yield and Tensile Strength vs. Strain Condition.

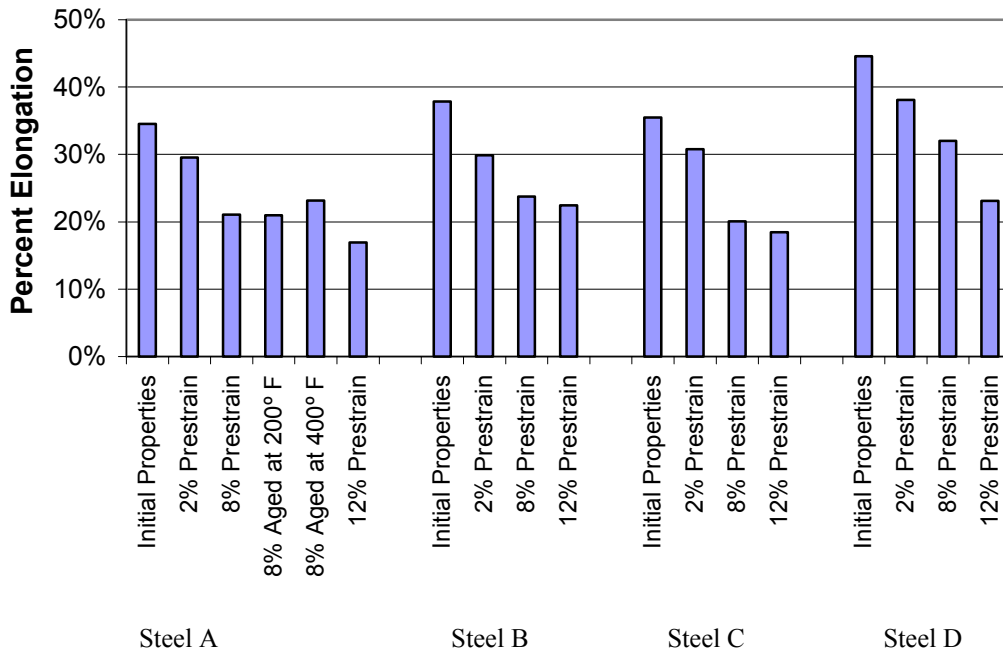


Figure 5 Summary of Tensile Elongation vs. Strain Condition.

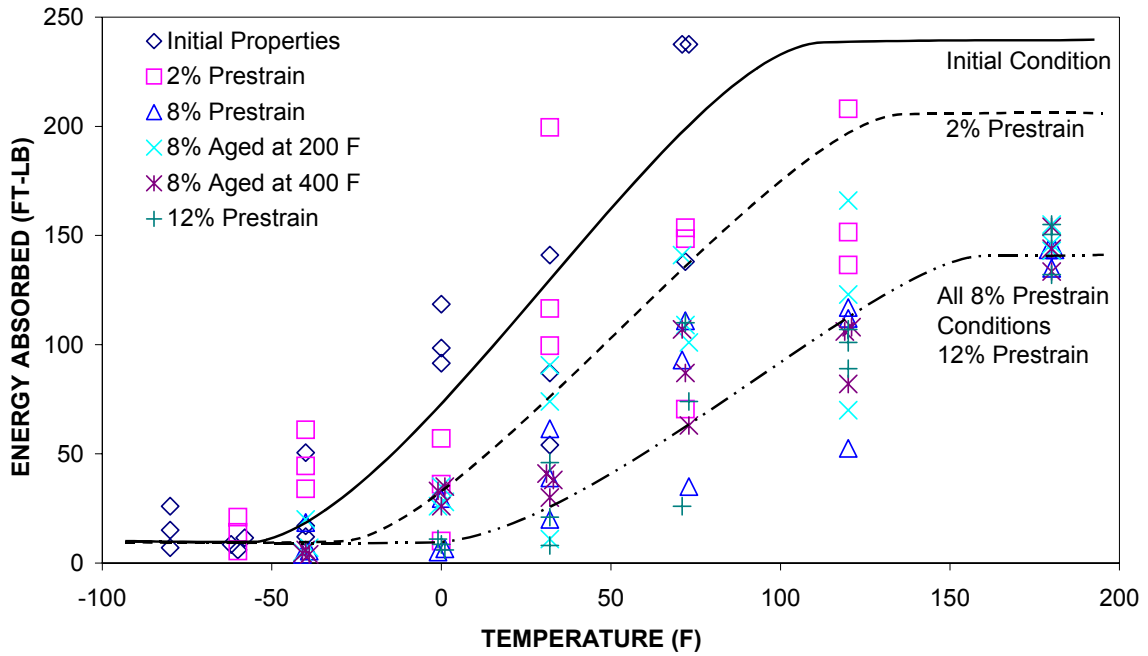


Figure 6A CVN Transition Curves (TL) For Steel A For Various Pre-strain Conditions.

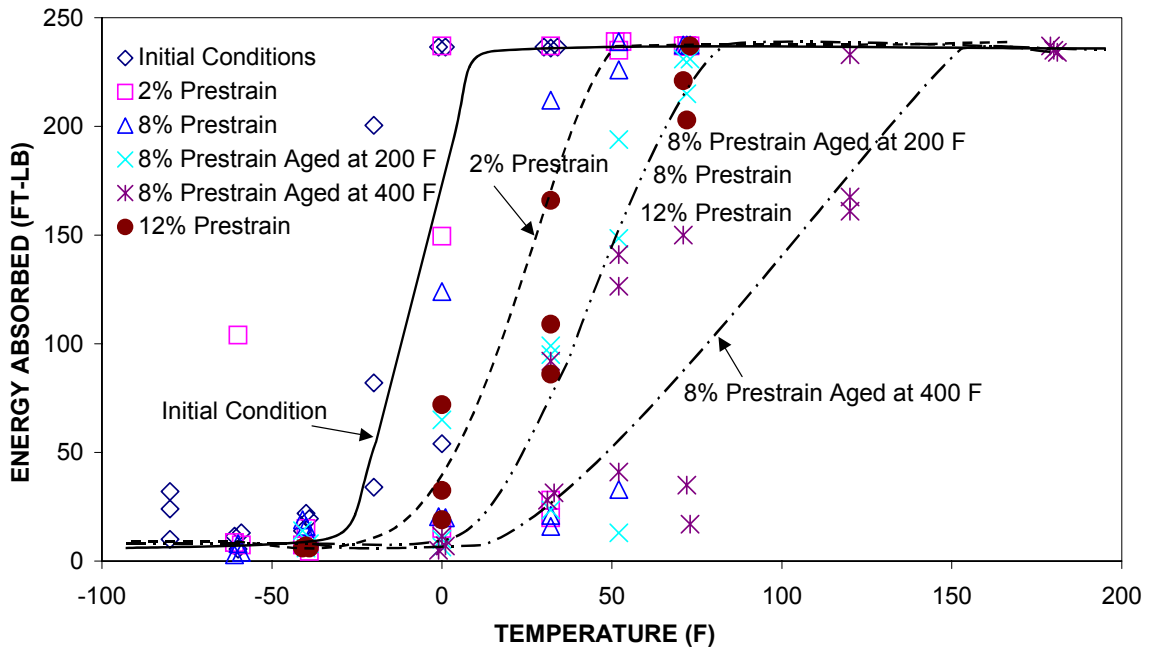


Figure 6B CVN Transition Curves (LT) For Steel A For Various Pre-strain Conditions.

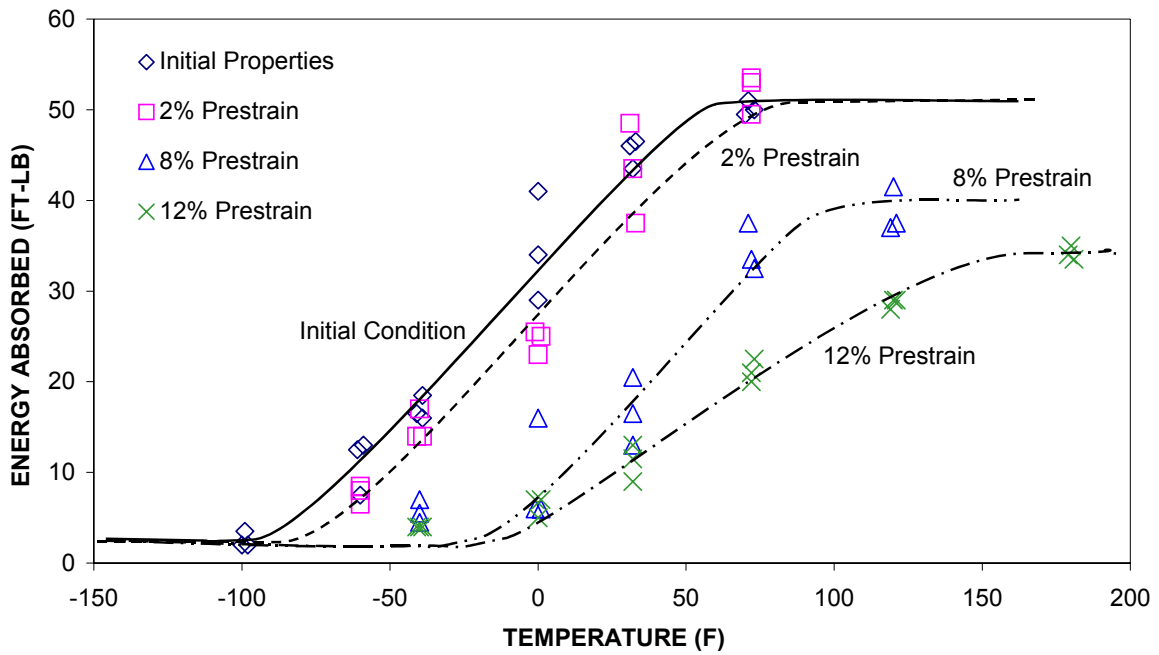


Figure 6C CVN Transition Curves (TL) For Steel B For Various Pre-strain Conditions.

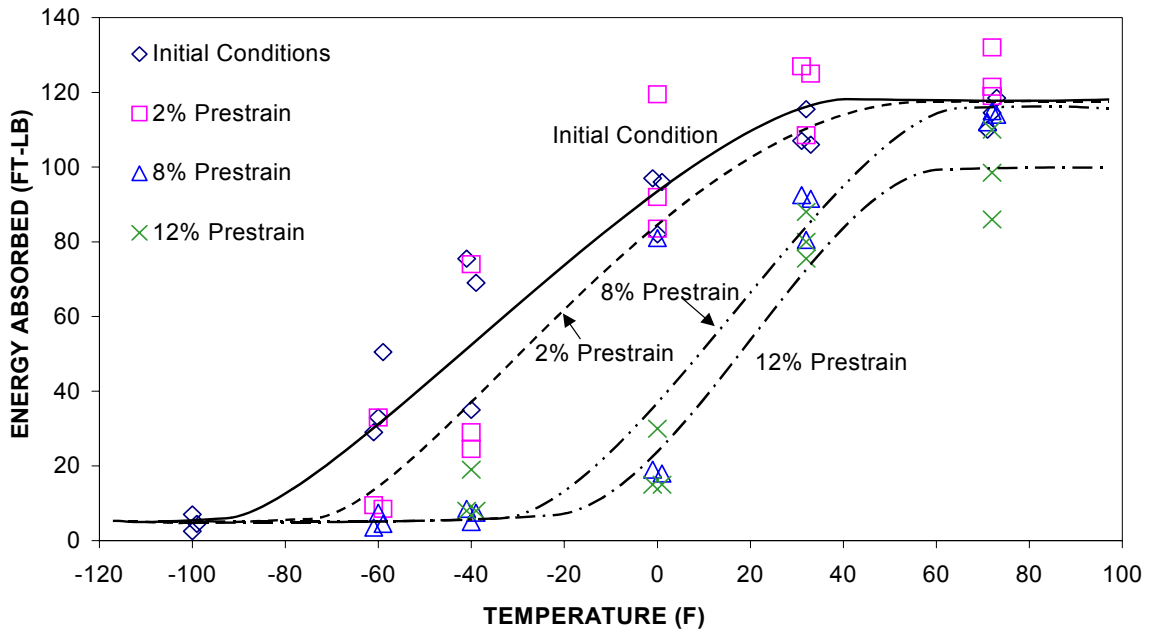


Figure 6D CVN Transition Curves (LT) For Steel B in the LT For Various Pre-strain Conditions.

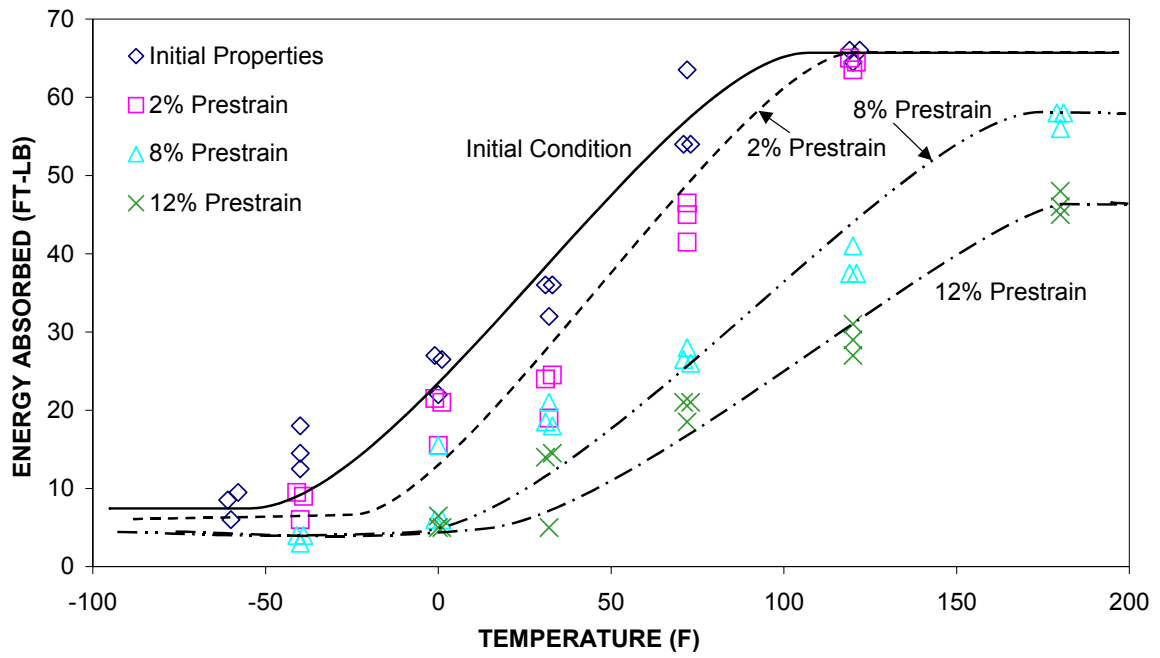


Figure 6E CVN Transition Curves (TL) For Steel C For Various Pre-strain Conditions.

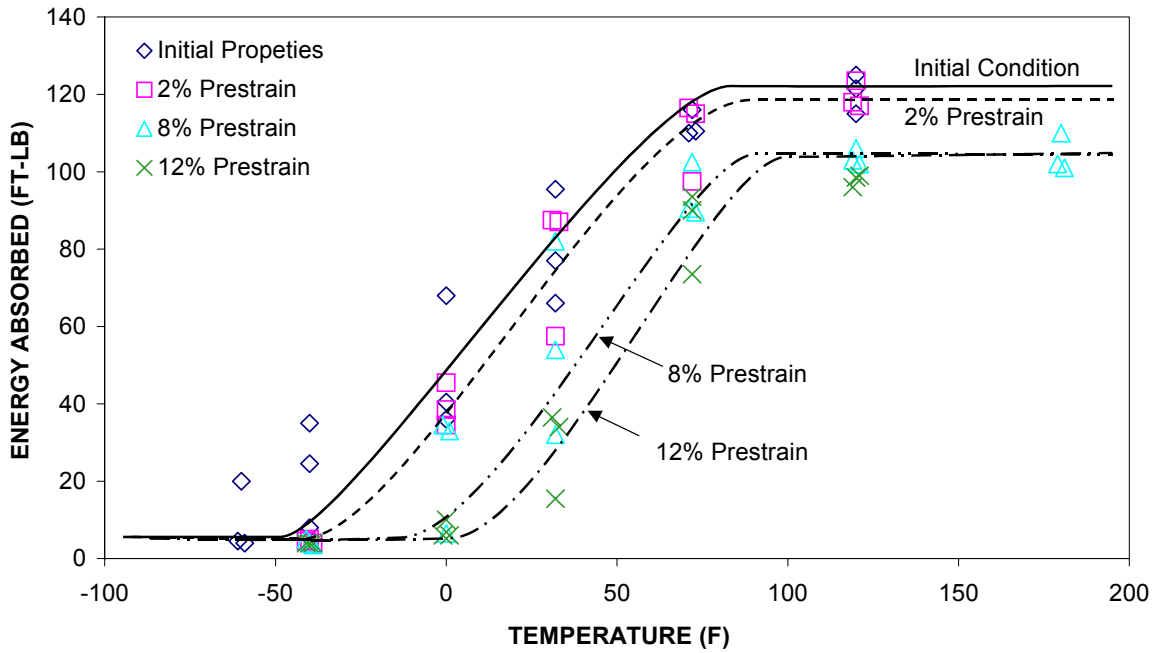


Figure 6F CVN Transition Curves (LT) For Steel C For Various Pre-strain Conditions.

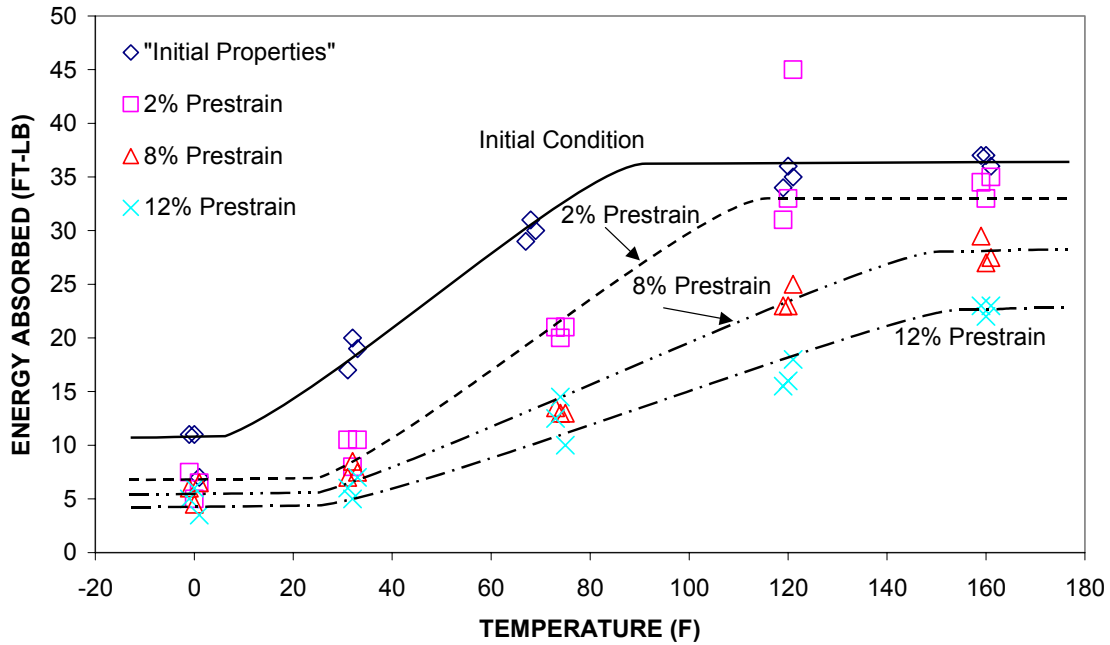


Figure 6G CVN Transition Curves (TL) For Steel D For Various Pre-strain Conditions.

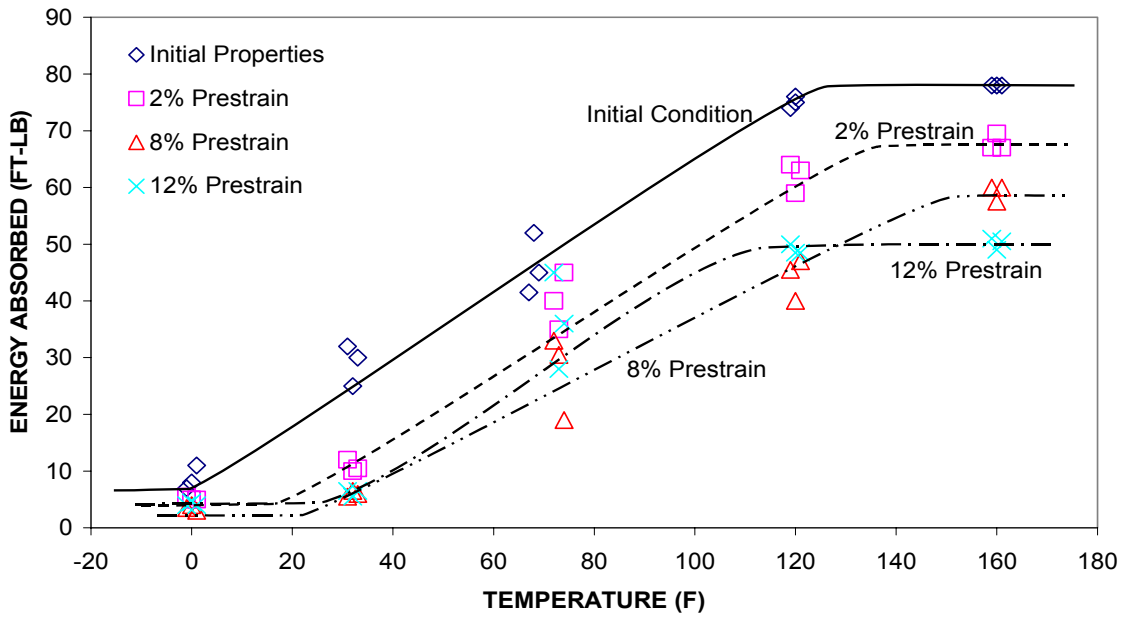


Figure 6H CVN Transition Curves (LT) For Steel D For Various Pre-strain Conditions.

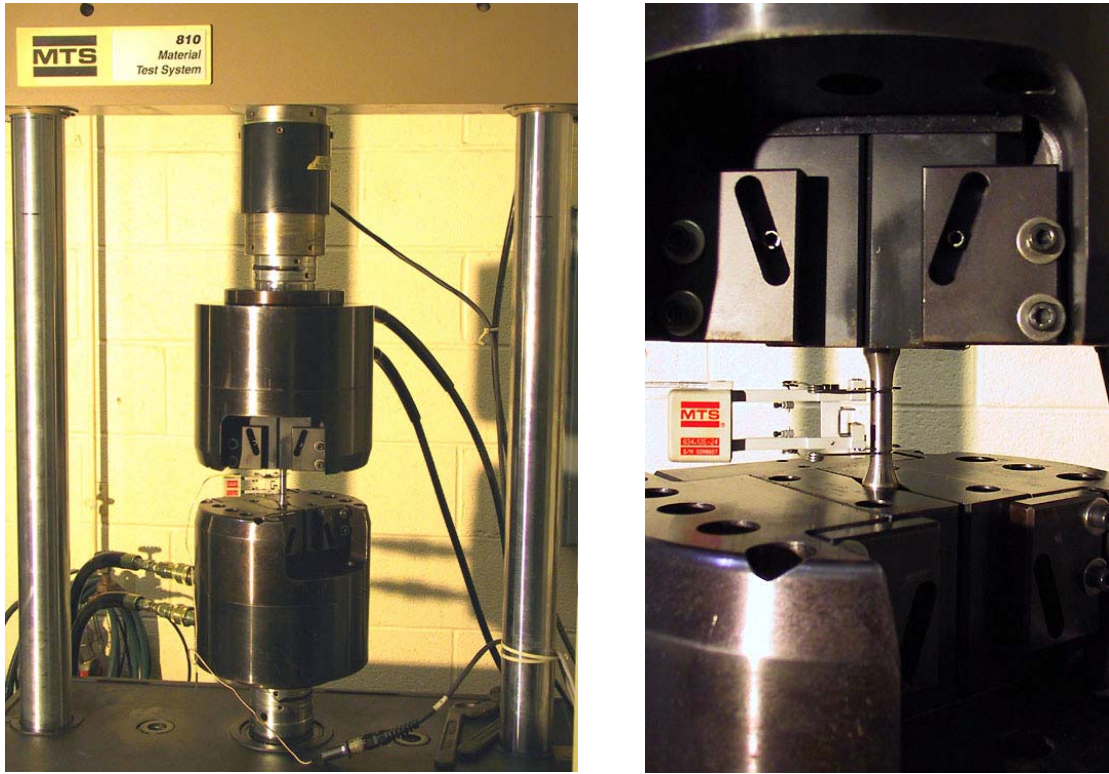


Figure 9 Cyclic Strain Test Set-up.

Steel D 4%

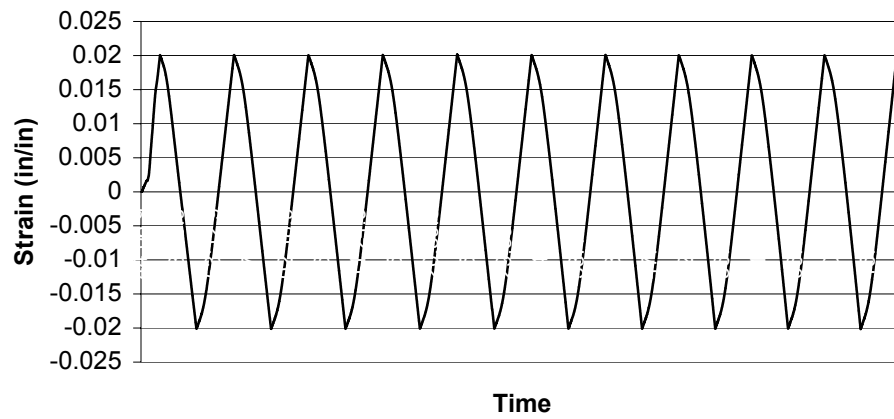


Figure 10 Typical Strain-Time Plot for a Single Cyclic Strain Test.

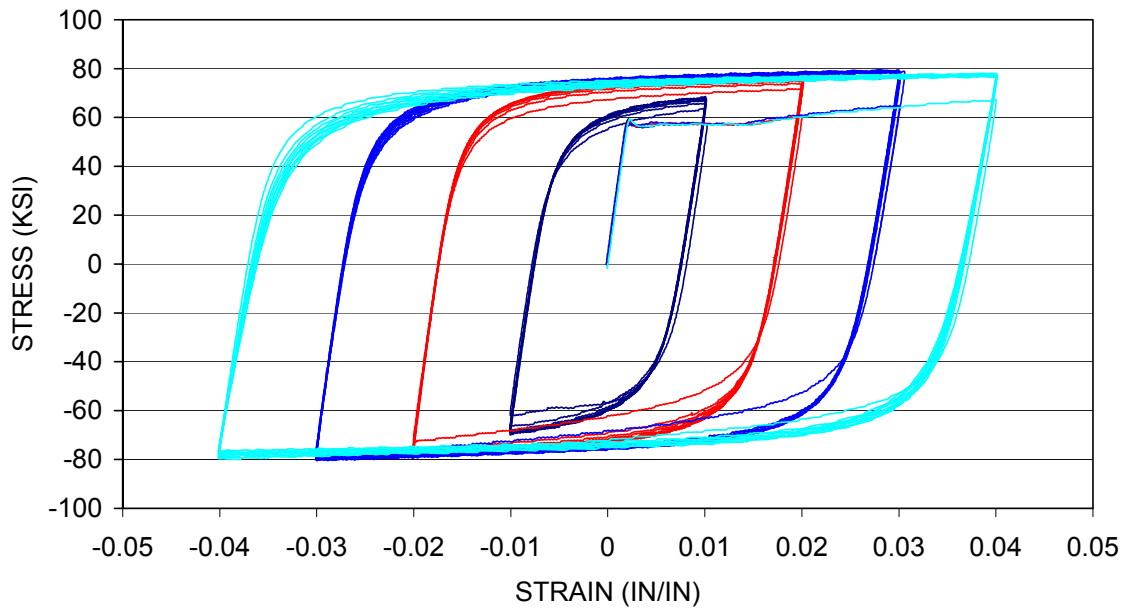


Figure 11A Composite Plot of Cyclic Strain Behavior of Steel A (10 cycles at 2%, 4%, 6%, and 8% Strain Range).

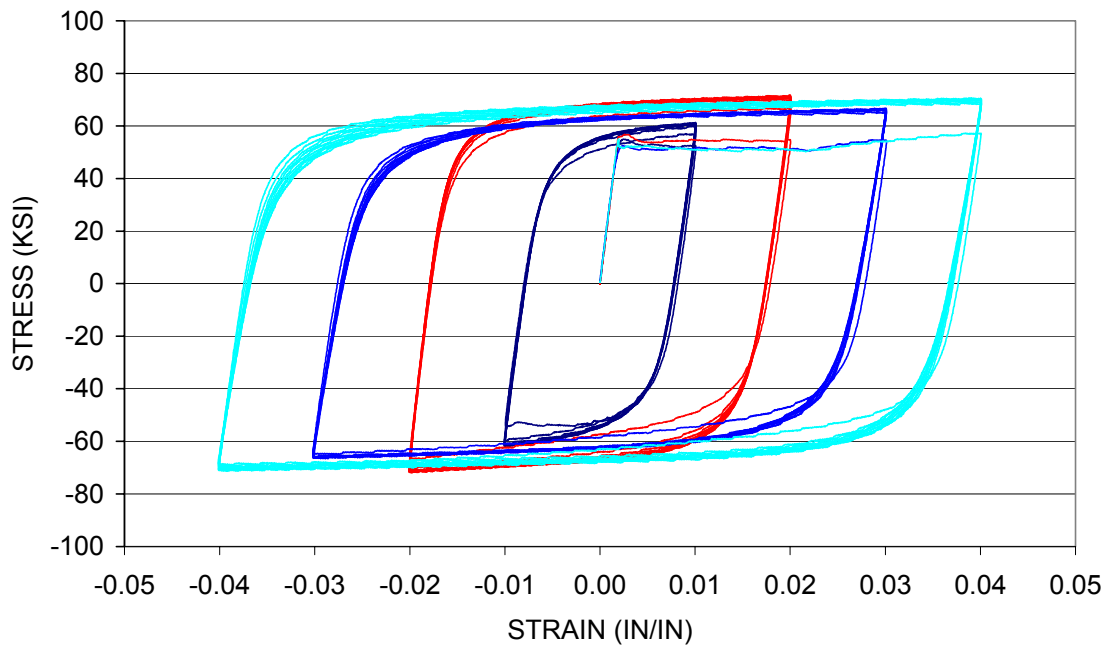


Figure 11B Composite Plot of Cyclic Strain Behavior of Steel B (10 cycles at 2%, 4%, 6% and 8% Strain Range).

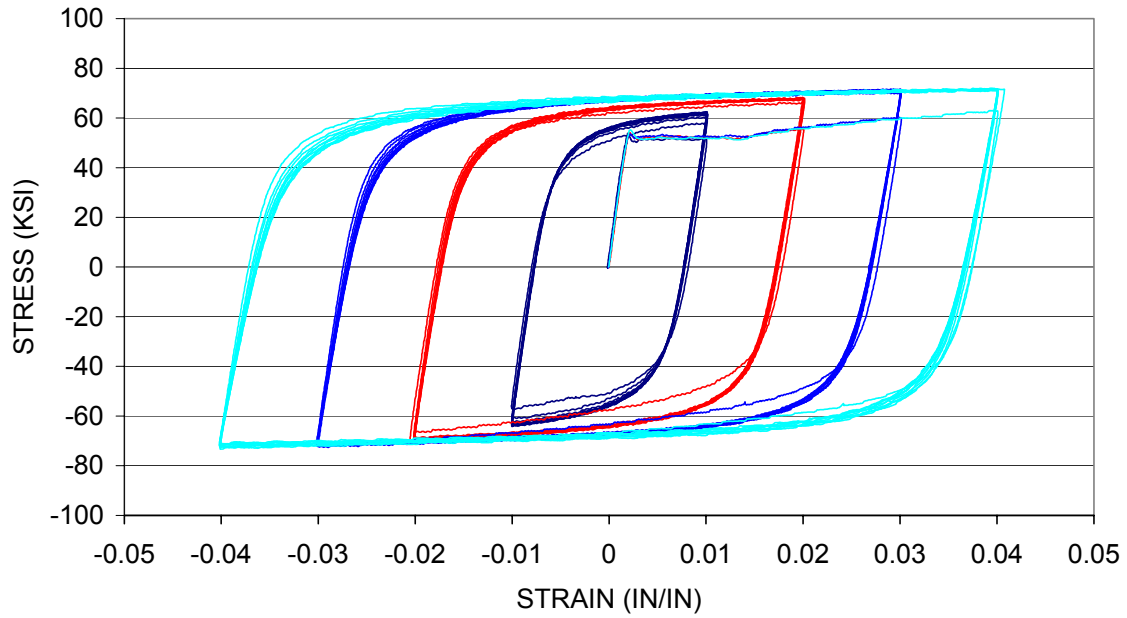


Figure 11C Composite Plot of Cyclic Strain Behavior of Steel C (10 cycles at 2%, 4%, 6% and 8% Strain Range).

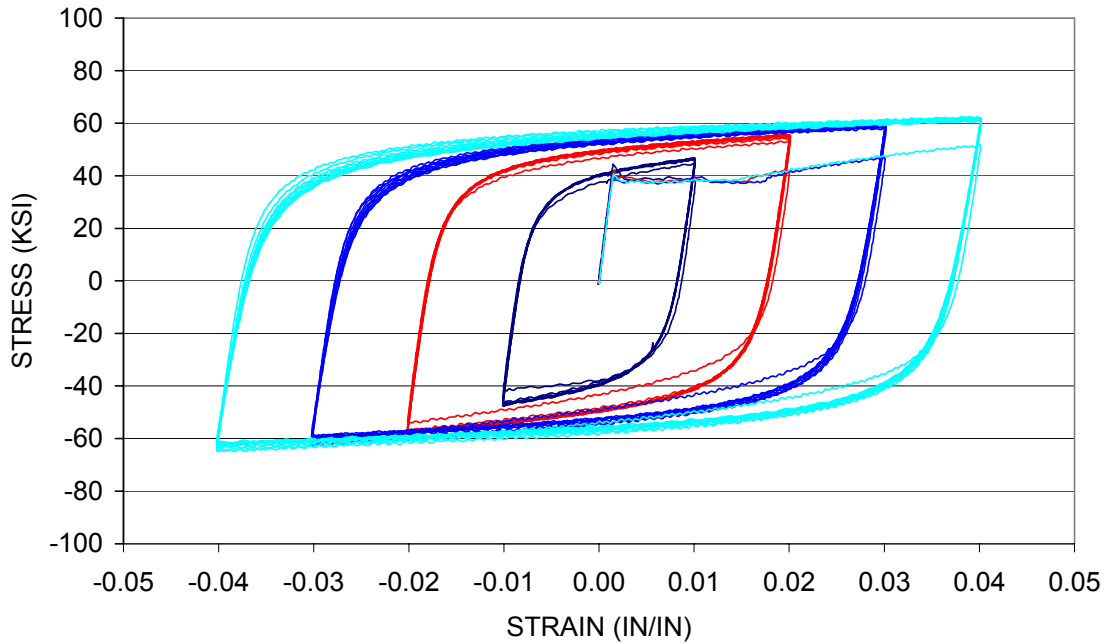


Figure 11D Composite Plot of Cyclic Strain Behavior of Steel D (10 cycles at 2%, 4%, 6% and 8% Strain Range).

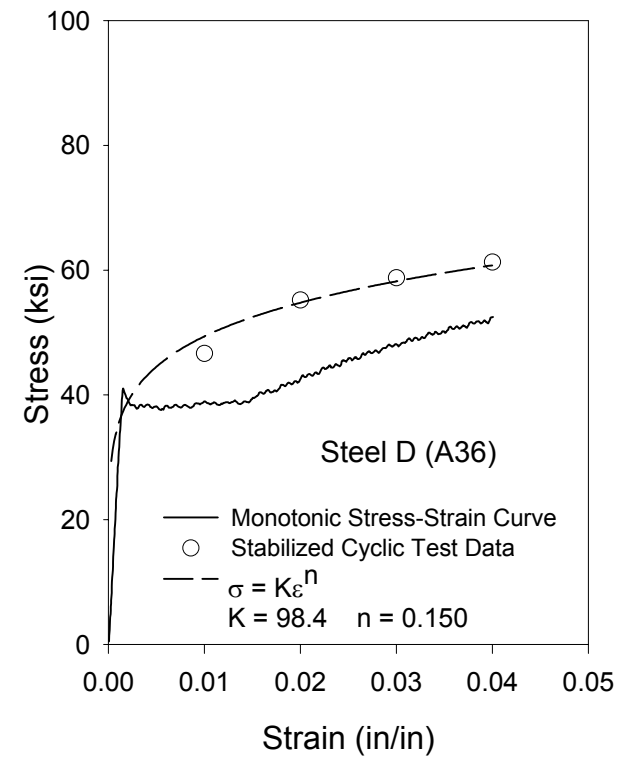
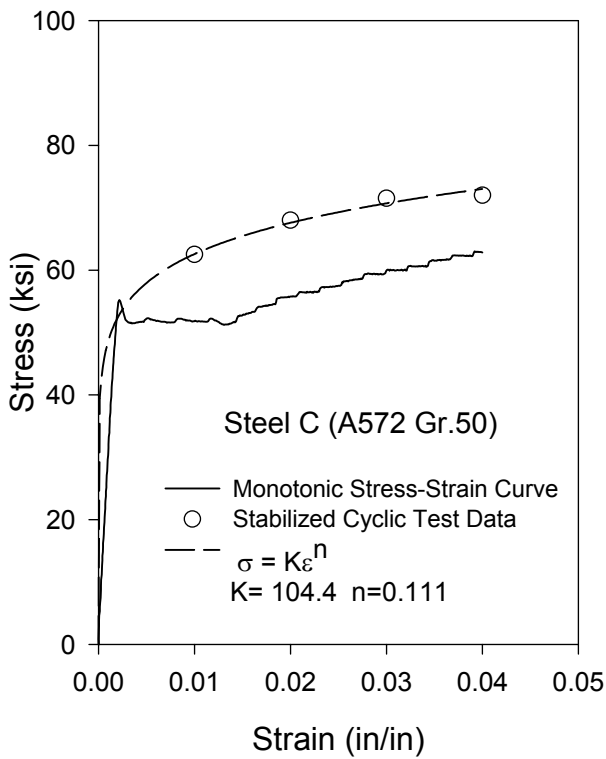
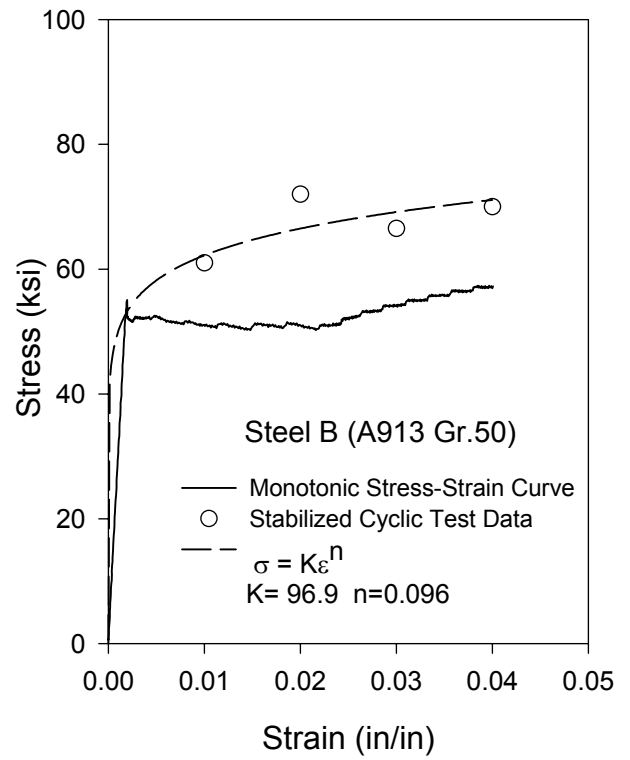
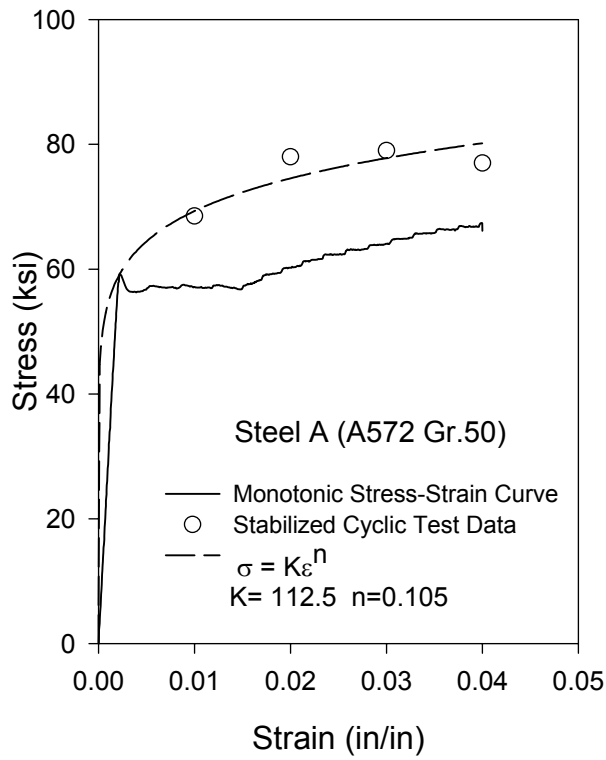


Figure 12 Comparison of Monotonic and Stabilized Cyclic Stress-Strain Behavior of the Four Steels.

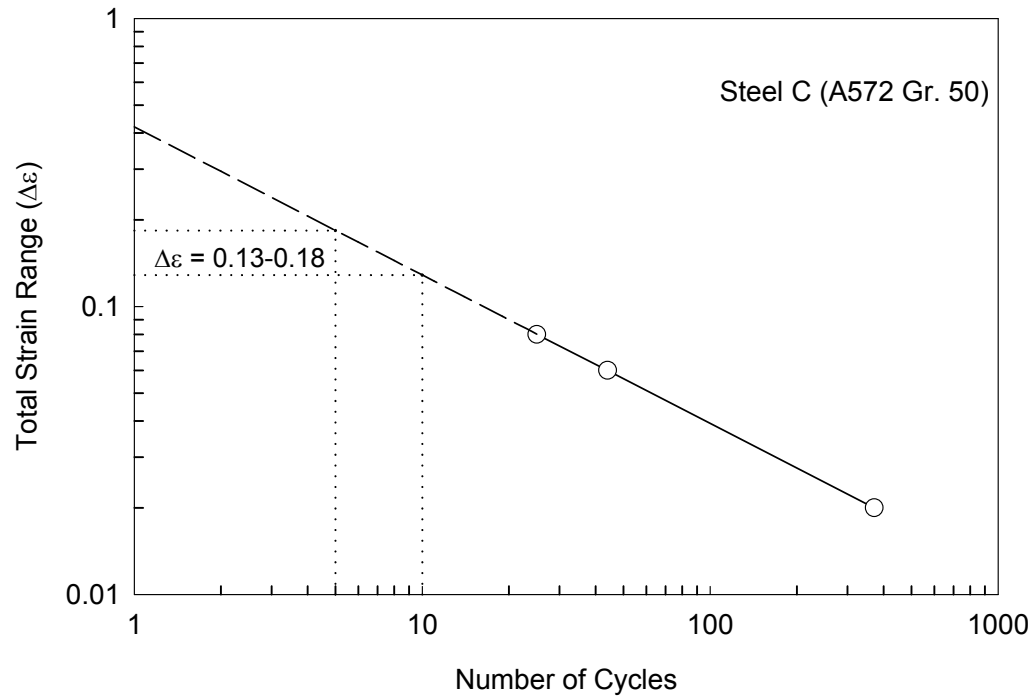


Figure 13 Strain-Life Plot for Steel C (A572 Gr. 50) with Data Extrapolated to Low Fatigue Life.